Two Modes of North American Drought from Instrumental and Paleoclimatic Data*

C. A. WOODHOUSE

Department of Geography and Regional Development, The University of Arizona, Tucson, Arizona

J. L. RUSSELL

Department of Geosciences, The University of Arizona, Tucson, Arizona

E. R. COOK

Lamont-Doherty Earth Observatory, Palisades, New York

(Manuscript received 2 July 2008, in final form 17 February 2009)

ABSTRACT

Droughts, which occur as a part of natural climate variability, are expected to increase in frequency and/or severity with global climate change. An improved understanding of droughts and their association with atmospheric circulation will add to the knowledge about the controls on drought, and the ways in which changes in climate may impact droughts. In this study, 1) major drought patterns across the United States have been defined, 2) the robustness of these patterns over time using tree-ring-based drought reconstructions have been evaluated, and 3) the drought patterns with respect to global atmospheric pressure patterns have been assessed. From this simple assessment, it is suggested that there are two major drought patterns across North America, which together account for about 30% of the total variance in drought patterns—one resembles the classic ENSO teleconnection, and the other displays an east–west drought dipole. The same two patterns are evident in the instrumental data and the reconstructed drought data for two different periods, 1404–2003 and 900–1350. The 500-mb circulation patterns associated with the two drought patterns suggest that the controls on drought may come from both Northern Hemisphere and tropical sources. The two drought patterns, and presumably their associated circulation patterns, vary in strength over time, indicating the combined effects of the two patterns on droughts over the past millennium.

1. Introduction

Drought is a feature of natural climate variability and a condition expected to be exacerbated by global climate change, particularly in the subtropical regions of the world (Arblaster et al. 2007; Seager et al. 2007). Droughts are receiving an increasing amount of attention in areas such as the western United States, where greater demands on water supplies due to increases in population, changing water demands, and recent droughts have converged, resulting in a heightened vulnerability to the impacts of drought (e.g., National Research Council 2007). Understanding the spatial and temporal characteristics of drought, and the controls on these characteristics, is critical to planning for and mitigating the impacts of regional drought. A great deal of research has been focused on improving this understanding over the past decades, utilizing information from instrumental and paleoclimatic data as well as climate modeling.

Spatial pattern of drought across North America have been investigated to identify both regions that tend to be homogeneous with respect to drought, and the spatial footprint of drought, such as those that characterized the 1930s Dust Bowl and 1950s droughts. The first study to address homogenous regions that incorporated data from the entire United States over the twentieth century defined nine distinct drought regions (Karl and Koscielny 1982). The nine regions had different frequency characteristics, with drought more persistent in the U.S. interior (Karl and Koscielny 1982), a finding that was

* Lamont-Doherty Earth Observatory Publication Number 7277.

Corresponding author address: C. A. Woodhouse, 412 Harvill Building, Box 2, Department of Geography and Regional Development, The University of Arizona, Tucson, AZ 85721-0076.
E-mail: conniew1@email.arizona.edu

DOI: 10.1175/2009JCLI2705.1

confirmed in further analysis (Karl 1983; Diaz 1983). Nine drought regions very similar to these were also identified in drought reconstructions based on moisture-sensitive tree-ring data, extending back to 1700 (Cook et al. 1999), an indication of the stability of these regions over time. The nature of wet and dry regimes in five areas representing regions of different synoptic-scale forcing across the contiguous United States was investigated by Diaz (1991). The regionally variable distribution of precipitation during wet and dry periods, as well as seasonal tendencies for initiation and termination, was suggested as an indication of both synoptic- and larger-scale circulation further modulated by seasonal atmospheric circulation and teleconnections (Diaz 1991; Barnston and Livesey 1987).

Spatial and temporal analyses of droughts and pluvials over the coterminous United States have been undertaken using highly resolved, gridded precipitation data [Parameter-Elevation Regressions on Independent Slopes Model (PRISM); Daly et al. 1997] for 1895–2003 (Kangas and Brown 2007). The increased spatial resolution of the data used in this study indicated a more heterogeneous coverage of droughts and pluvials than suggested by some previous studies. Results showed dependence on the time scales used to define drought, with short-duration droughts characterized by high temporal and spatial variability, and large areas under drought for very short periods (e.g., a month), while droughts evaluated at longer time scales, such as 12- and 24-month periods, showed more persistence. Indices of short-term droughts indicated a higher frequency of drought in the interior United States, as well as more spatially extensive droughts and pluvials in this region, compared to other regions. More severe extremes occurred in western and some eastern parts of the United States (Kangas and Brown 2007).

Links between the spatial patterns of drought and the mechanisms that control drought have been the topic of much research. El Niño–Southern Oscillation (ENSO) was the first large-scale ocean–atmosphere mechanism to be linked to drought (e.g., Rasmussen and Carpenter 1982; Glantz et al. 1991). ENSO has a distinct footprint on drought in North America (e.g., Cayan 1996; Redmond and Koch 1991), which can also be quite spatially variable (Cole and Cook 1998; Rajagopalan et al. 2000; Brown and Comrie 2004). The interplay between low-frequency and high-frequency variations in Pacific Ocean variability has been shown to be influential to regional climate and drought conditions in North America, resulting in enhanced or diminished regional drought occurrence and severity (Gershunov and Barnett 1998; Barlow et al. 2001; Brown and Comrie 2004; Shabbar and Skinner 2004). Analysis of spatial patterns of U.S. drought associated with the main modes of decadal-scale variability in both the Atlantic and Pacific Oceans suggests that a warm Atlantic, conditioned by Pacific Ocean SSTs, is linked to widespread droughts such as those of the 1930s and 1950s (McCabe et al. 2004). Most recently, modeling studies have further indicated the role of both the North Atlantic and the tropical Pacific in promoting North American drought (Seager et al. 2008; Feng et al. 2008).

Patterns of North American drought have been explored with a rich archive of paleoclimatic data, including tree-ring-based gridded drought reconstructions for North America (Cook et al. 1999, 2004). In addition to defining drought regions (Cook et al. 1999), these and other paleoclimatic data have been used to examine spatial patterns of drought over the past millennia. A number of studies document droughts more persistent and severe than those that have occurred during the period of instrumental records (e.g., Woodhouse and Overpeck 1998; Stahle et al. 1998, 2000; Benson et al. 2002; Cook et al. 2004). An assessment of the spatial analogs of the 1930s and 1950s drought in the context of the past five centuries provided an estimated return interval of 45 yr for a 1950s-type drought (Fye et al. 2003). Millennial-length North American drought reconstructions document drought of unprecedented persistence during the medieval period, but with spatial patterns that are similar to those of twentieth-century droughts (Herweijer et al. 2007). The primary spatial footprint of these medieval droughts implies ENSO as a causal mechanism, and additional modeling and other paleoclimatic data support the important role of persistent and cool tropical Pacific SSTs in these periods of extended drought (Seager et al. 2005; Herweijer et al. 2007; Cook et al. 2007; Graham et al. 2007).

Although far from a complete assessment of the literature, this review documents the rich body of knowledge that supports our understanding of the major drought regions in the United States, the general footprint of major droughts, and possible causal mechanisms. Much research points to the key role of the tropical Pacific Ocean, with indications of the importance of the North Pacific and Atlantic Oceans as controls on regional patterns of drought as well. In this study we take advantage of the gridded North American drought reconstructions for the past millennia to investigate major patterns of drought over three time periods—the twentieth century, the last 500 yr, and the medieval period. Instead of looking for the spatial footprint of the major twentieth-century droughts or the characteristic imprint of known circulation mechanisms on patterns of drought, we let the data define the major patterns, and then draw inferences about the causal

FIG. 1. PDSI grid points used in this study, based on a network of 286 points in a 2.5° × 2.5° grid over North America for both instrumental and reconstructed data (updated from Cook et al. 2004; NOAA/National Climatic Data Center 2008a). Reconstruction data and methods are described in Cook et al. (2004) and associated online supporting materials. (a) Black outline indicates grid points with the common period 1404–2003, selected for the best spatial coverage over the longest period of time; gray shading indicates data points not used in the instrumental data analysis, 1900–2003 (data for non-U.S. points not available to 2003). (b) Inset shows grid points used for the 900–1350 analysis (outlined, nonshaded points).

mechanisms that are associated with these patterns. This approach allows an evaluation of droughts that are identified first in terms of spatial patterns, and then by their association with the atmospheric circulation, rather than examining drought anomaly patterns related to associations with circulation indices. We use gridded instrumental drought data to identify major spatial patterns of drought across the coterminous U.S. and border regions, followed by a similar analysis using reconstructed drought data to assess the robustness and stability of these patterns over two time periods: 1404–2003, and 900–1350, also known as the Medieval Climate Anomaly (e.g., Cook et al. 2004). We then investigate the association between the spatial patterns of drought and atmospheric circulation (500-mb geopotential heights) patterns to infer possible driving mechanisms. Finally, we examine the reconstructed drought patterns for the two time periods to assess the possible role of circulation over time.

2. Data and methods

The two gridded drought datasets for North America used in this study are based on the summer (June–August) Palmer Drought Severity Index (PDSI; Palmer 1965). The PDSI has a lag incorporated into its calculation that results in the summer PDSI reflecting drought conditions of previous seasons (Cook et al. 1999). The PDSI datasets used are from Cook et al. (2004, updated version available online at http://www.ncdc.noaa.gov/paleo/pdsi_ts.html; NOAA National Climatic Data Center 2008a) and are based on a network of 286 points in a 2.5° × 2.5° grid over North America. The instrumental dataset extends from 1900 to 2003, while the tree-ring-reconstructed PDSI extends back 350–2000 yr, depending on location (with the variance adjusted to match the instrumental data in the twentieth and twenty-first centuries). A subset of these data was used for this study. For the reconstruction data, the grid points with the common period 1404–2003 were selected for the best spatial coverage over the longest period of time. The set includes most of the U.S. and bordering parts of Canada and Mexico (Fig. 1). Several grid points from the Great Lakes region and southern Florida were omitted because of the lower validation statistics compared to the instrumental data. A sparser set of grid points was used to examine the medieval period (Fig. 1, inset). For the instrumental data, the same grid points were used as for the 1404–2003 reconstruction dataset, but were restricted to those with the common years 1900–2003 (which excluded the non-U.S. grid points). A total of 160 grid points was retained for the 1404–2003 reconstructed

dataset, 128 for the 900–1350 reconstructed dataset, and 137 grid points for the instrumental dataset (Fig. 1). For the investigation of circulation patterns associated with drought patterns, monthly global 500-mb pressure data from the National Centers for Environmental Prediction–National Center for Atmospheric Research (NCEP–NCAR) reanalysis were used (Kalnay et al. 1996). The average for December through March was selected to represent cold season conditions. Drought patterns in the instrumental data were identified using T-mode principle components analysis (PCA) with a normalized Varimax (orthogonal) rotation (Richman 1986; Yarnal 1993). A T-mode PCA, based on a matrix with columns of years and rows of PDSI gridpoint values, yields principle components (PCs) characterized by years with similar spatial patterns. This approach differs from some previous studies that used PCA to identify drought regions by grouping data spatially (e.g., Karl and Koscielny 1982; Cook et al. 1999). In this study, the focus is not on regions that behave similarly with respect to drought, but on identifying the primary spatial patterns, or footprints, of drought across North America. The number of PCs rotated was based on a cutoff of eigenvalues >1.0 (although several different cutoffs were tried with the same resulting patterns). Scree plots were used to further screen components for analysis. For the analysis of reconstructed PDSI, T-mode PCA with same numbers of PCs rotated was repeated. Composite maps of the five noncontiguous years with the largest positive and negative loadings for the main PCs were used to illustrate spatial patterns of drought for the instrumental period and two paleoperiods. Years in the reconstructed data that also ranked in the top five for the instrumental data were replaced with the next highest ranking year so that the patterns for reconstructed and instrumental periods were independent. This approach is roughly analogous to Blasing's (1975) correlation map–based identification of twentieth-century patterns of surface pressure types, but differs in that years of pressure anomaly types were the basis for the composite precipitation, temperature, and tree-ring-width maps, while here we are using the gridded PSDI to identify patterns in both the instrumental and reconstructed data. The composite maps were generated using data and maps from the National Oceanic and Atmospheric Administration (NOAA)/National Climatic Data Center (2008b) using the full gridded PDSI dataset. To summarize, PC loadings represent time series of the leading drought patterns, while the composite maps of the years with the largest loadings are used to represent the corresponding leading spatial patterns of drought. Time series of the PC loadings were used to explore the relations between PCs over time. The association between drought patterns and atmospheric circulation was examined using correlation maps with PC loadings and global 500-mb heights, 1949–2003 (sea level pressure correlation maps were generated as well, with very similar results). To assess the consistency of the patterns depicted in the composite maps over the three time periods, we also generated maps from the PC scores [analogous to spatial patterns from empirical orthogonal functions (EOFs)]. The PC scores were generated from a normalized varimax rotation in which factor loadings are divided by the square roots of the respective communalities (StatSoft, Inc. 2005).

3. Results

a. Drought patterns in the instrumental and paleodrought data

The PCA, which grouped the PDSI map patterns for the years 1900–2003 into years with similar patterns, resulted in 15 PCs with eigenvalues greater than 1.0. After rotation of the 15 PCs, the first two PCs explained 16% and 14% of the total variance, respectively, and they were targeted for further analysis. When the eigenvalue sampling error is compared to the spacing of eigenvalues assessed using North's rule of thumb (North et al. 1982), the two PCs appear to be separate and unmixed with each other. The loadings of these two PCs were ranked and the five noncontiguous years with the highest negative and positive loadings were used to generate composite maps to illustrate the main spatial features of the two PCs. The composite map for PC1 shows a Pacific Northwest–southwestern U.S. dipole (Fig. 2a, left), a characteristic of the ENSO imprint on the western United States (Dettinger et al. 1998). An examination of the Southern Oscillation index November–March averages (NOAA/Climate Prediction Center 2008) indicates that positive PC1 values coincide with 10 out of the 15 strongest positive SOI years (indicating cool ENSO events) and negative PC1 values correspond with 9 of the 15 most negative SOI winters (indicating warm ENSO events). PC2 displays an eastern–western U.S. drought dipole that is indicative of highly meridional flow (Fig. 2a, right). The reconstructed PDSI data, analyzed for the same years (1900–2003) show the same spatial structure in the first two PCs as the instrumental data (Fig. 2b). The top ranking 5 yr are not identical for both the instrumental and reconstructed data over this common period (cf. Figs. 2a and 2b), but the reconstruction years that are not the same as the instrumental years rank in the top 20% of years in the instrumental analysis (and all but two in the top 15%).

The sensitivity of these patterns to data treatment was assessed by retaining different numbers of PCs for

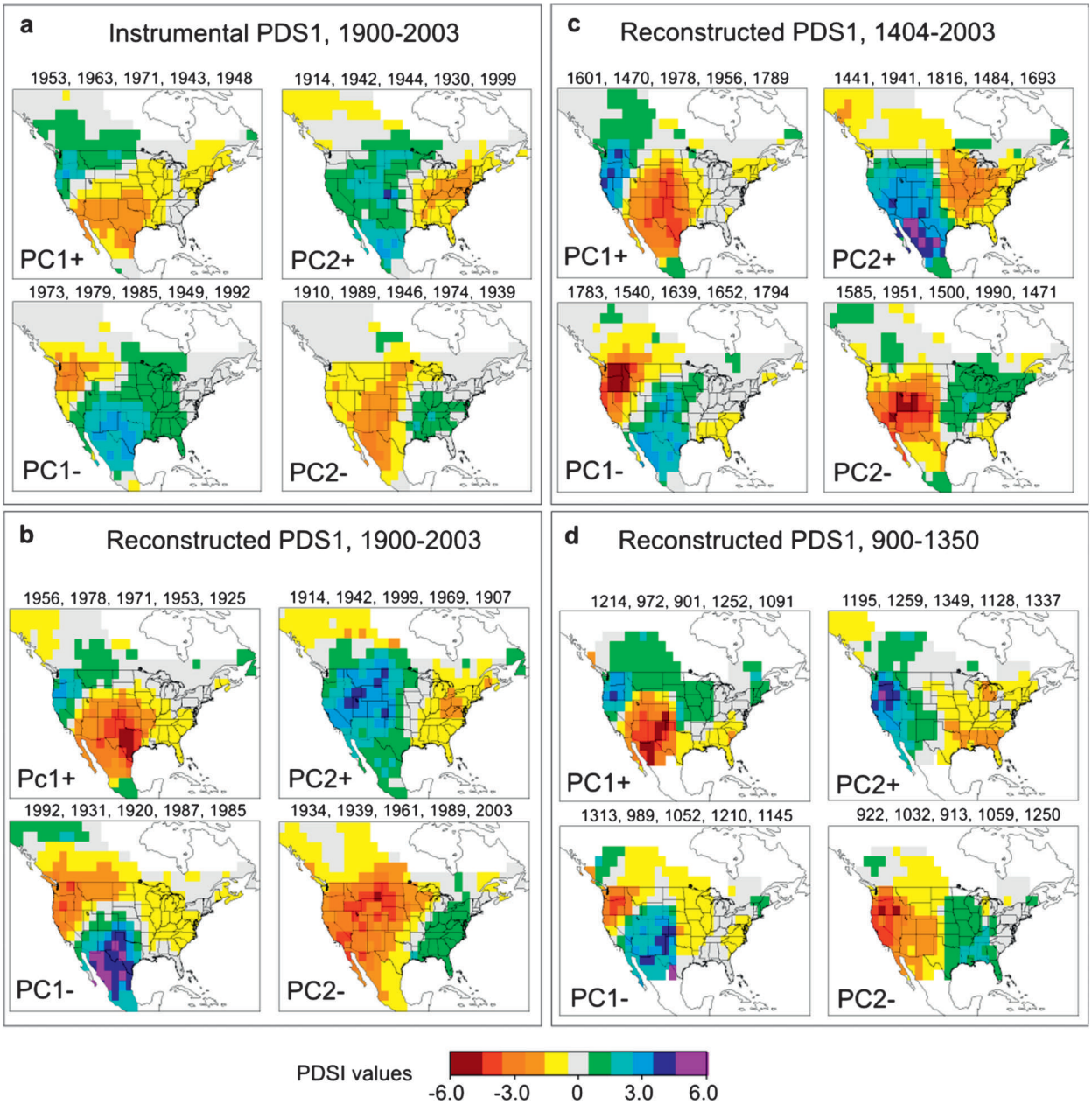

FIG. 2. Composite maps for five noncontiguous years with highest negative and positive loadings, (left) PC1 and (right) PC2, for each set. (a) PCA on instrumental PDSI, 1900–2003. (b) PCA on reconstructed PDSI, 1900–2003. (c) PCA on reconstructed PDSI, 1404–2003. (d) PCA on reconstructed PDSI, 900–1350. The composite maps were generated using the full gridded PDSI dataset.

rotation (nine and five), and by generating composite maps using drought datasets that used different spatial interpolation approaches [NOAA/National Climatic Data Center (2008c) Divisional PDSI and Dai et al. (2004) gridded PDSI]. Resulting maps were all very similar, sharing the southwest–northwest and east–west dipole patterns and most of the same five highest ranking years.

To further test the stability of these two drought patterns, the reconstructed PDSI data with years prior to the twentieth century were subject to the same PCA process. As with the instrumental data, 15 PCs were rotated, and the composite maps of the five highest ranking years for first two PCs were generated. The PCA process was run first on the years 1404–2003 (Fig. 1a), and then on a smaller subset of the gridded data for the years 900–1350 (Fig. 1b). In both cases, as with the instrumental data, the two PCs appear to be separate from each other (North et al. 1982). In the period 1404–2003,

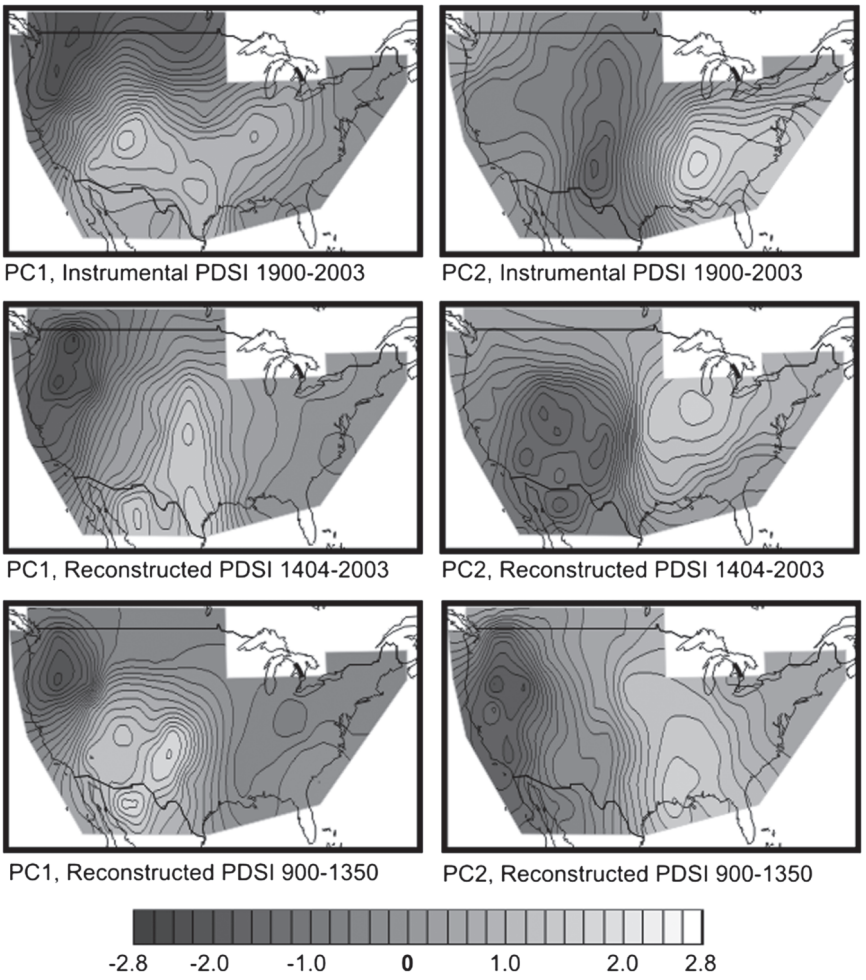

FIG. 3. Maps based on PC scores for (top) instrumental PDSI, 1900–2003, (middle) reconstructed PDSI, 1404–2003, and (bottom) reconstructed PDSI, 900–1350: (left) PC 1 and (right) PC 2.

the first two PCs explained 17% and 18% of the total variance, respectively, while explaining 21% and 14% of the total variance, respectively, for the 900–1350 period. The resulting map patterns were very similar for both the 1404–2003, and 900–1350 periods (the sign of the loadings for both reconstruction periods were reversed for PC1, and for PC2 for the 1404–2003 period, relative to the signs of the instrumental PC loadings; these have been changed in the figures to facilitate comparison; see Figs. 2c,d). The patterns for PC1 are the most consistently similar, especially with regard to western North America. In the medieval period, the pattern over the Midwest is different, but this could be due, at least in part, to the less complete data coverage over this region during this time (see Fig. 1b). The PC2 patterns are characterized by an east–west split in the general vicinity of the Great Plains. The spatial patterns based on the full time series for each of the three time periods, resulting from the PC scores, are very similar (Fig. 3).

The time series of the loadings for the period of time common to the instrumental and reconstructed PDSI PCs were compared to assess the skill of the reconstructed data in replicating the temporal as well as spatial patterns of the instrumental PDSI data (Fig. 4). The loadings were inverted where necessary so that negative values for PC1 indicate dry Southwest and wet Northwest conditions, while negative values for PC2 indicate dry west and wet east conditions (and the reverse for the positive loadings). The time series of the reconstruction loadings closely match the instrumental data. The correlations between instrumental and reconstructed PCs (unsmoothed) are $r = 0.830$ for PC1 and $r = 0.657$ for PC2. The higher correlation for PC1 is likely due to the close match with the instrumental PC from about

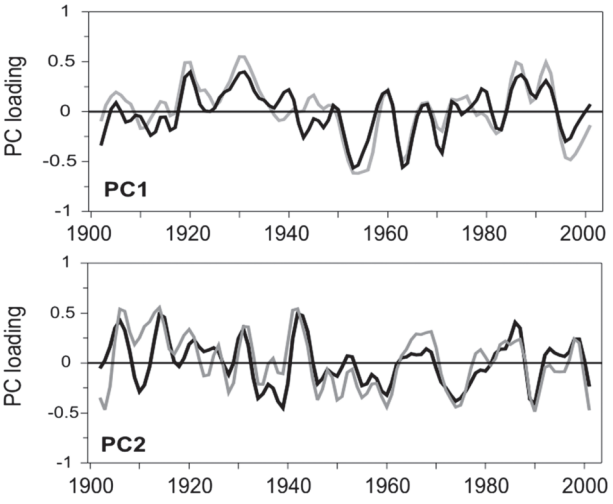

FIG. 4. Instrumental (black lines) and reconstructed (gray lines) PCs (top) 1 and (bottom) 2, 1900–2003, with five-point binomial filter. Loadings have been inverted where necessary so that negative values of PC1 indicate dry southwest–wet northwest and negative values of PC2 indicate dry west–wet east. Positive values are the opposite.

1950 to 1970, when southwestern U.S. droughts of the 1950s and 1960s were very well replicated.

The correlation between the rotated loadings for the PCs shows very a very weak statistically significant relationship between PC1 and PC2 for the analysis period, 1404–2003 ($r = -0.089$, $p < 0.05$), but not for the other two periods. The scores for the two PCs for all three time periods are uncorrelated. Statistically speaking, there is a chance that the two PCs are related to each other during the 1404–2003 period. In reality, such a relationship would not be unexpected, as is discussed in section 4.

b. Drought and atmospheric circulation

Correlation maps of the loadings for the two PCs and global 500-mb heights show the associations between the leading drought patterns and global circulation. The correlation map for PC1 features centers of negative correlation west of the Aleutian Islands and off Southern California and Baja, and positive correlations in the western North Pacific, over northern and eastern North America, and in the eastern North Atlantic (Fig. 5a, top). If shifted east, the two strongest centers of negative correlation would roughly approximate the Aleutian low and Northern Hemisphere 500-mb pattern corresponding to ENSO. The pattern is somewhat more similar to the western Pacific pattern of Wallace and Gutzler (1981) in their set of major teleconnection patterns identified during Northern Hemisphere winters (Figs. 5a,b, top), which is linked to equatorial Pacific conditions (Horel and Wallace 1981).

The main feature of the PC2 map is a center of negative correlation over Hudson Bay and extending east beyond the southern end of Greenland (Fig. 5a, bottom). A weaker center of negative correlation lies over central Asia. Positive correlations are centered over southeastern Europe and also stretch from eastern Siberia across the North Pacific Ocean. This pattern of correlations over northern latitudes is more indicative of the Arctic Oscillation pattern of 500-mb heights, which is dominated by a center of low pressure centered over Greenland, with high pressure stretching from eastern North America to central Europe, and over northeastern Asia. (Figs. 5a,b, bottom).

The circulation anomaly patterns associated with the two PCs do share a center of anomalous pressure off the coast of California. Negative PC1 (dry Southwest) and positive PC2 (dry west) are both associated with high pressure, but the pressure centers are in somewhat different locations. The center associated with PC1 is off the coast of Southern California and Baja, which would block flow into the southwestern United States, corresponding well to the southwestern–northwestern drought dipole pattern. The pressure anomaly off the coast of central to northern California in the PC2 pattern could lead to more west-wide drought, in agreement with the PC2 east–west drought dipole pattern. However, other features in the two anomaly patterns are rather different, which suggests there are two different sets of circulation patterns associated with the west coastal centers of high pressure for PC1 and PC2 droughts.

4. Discussion

The drought map patterns and the 500-mb correlation maps suggest two different North American drought patterns, and two types of circulation features associated with these two patterns that may be influencing drought across North America. The map pattern for PC1 shows a classic ENSO-type signature, and the corresponding correlation map shows the relationship between North American drought patterns and atmospheric circulation that could be expected from ENSO. ENSO has been shown to be a main driver of North American drought, so this result is not unexpected. The second PC is more strongly indicative of a Northern Hemisphere control on drought. The east–west dipole suggests meridional flow across the continent that is typically controlled by the position of the polar jet stream and the Rossby waves that influence its path (Barry and Chorley 2003). The correlation map supports a Northern Hemisphere annular mode (NAM) type of pattern, with centers of one sign over southern Greenland and the opposite sign over the Mediterranean (Thompson and Wallace 2000). Correlations between the PCs and the Southern Oscillation index

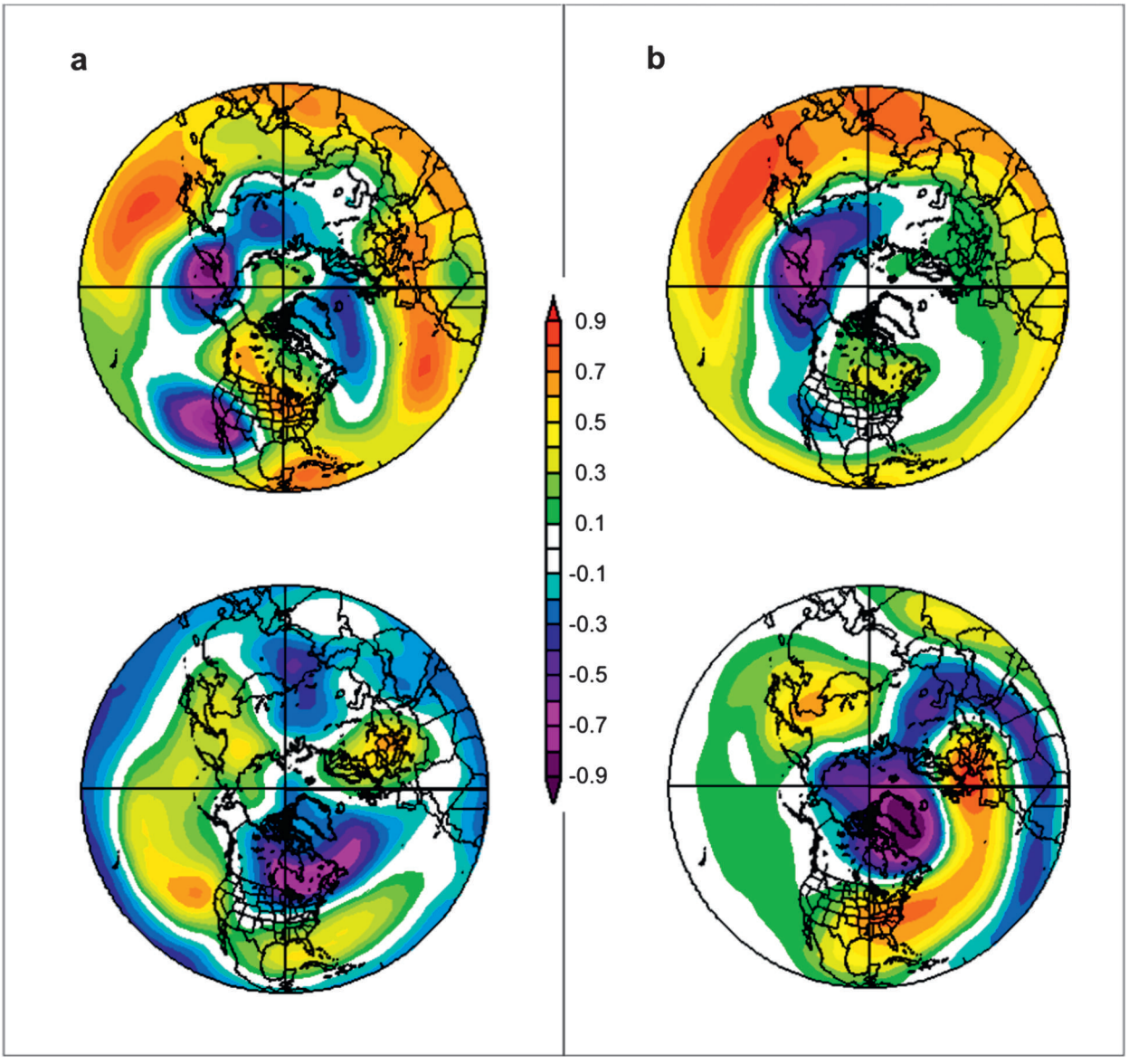

FIG. 5. (a) Correlation fields for December–March 500-mb heights and PC loadings: (top) PC1 and (bottom) PC2. (b) Correlation fields for December–March 500-mb heights and (top) western Pacific index (Wallace and Gutzler 1981) and (bottom) Arctic Oscillation (Thompson and Wallace 2000), 1949–2003. Images provided by NOAA/Earth System Research Laboratory (2008).

(NOAA/Climate Prediction Center 2008) and the Arctic Oscillation index (Thompson and Wallace 1998; data obtained from NOAA/Climate Prediction Center 2008), however, do not indicate a clear association based on these circulation indices, suggesting that the relationship is not a simple teleconnection. The two patterns—ENSO type and NAM type—do correspond well to the two main patterns of Northern Hemisphere winter climate variability identified by Quadrelli and Wallace (2004), related to the NAM and the Pacific–North American (PNA) pattern, with PNA representing an EOF that includes the Southern Oscillation index. If these two PCs do indeed represent major patterns of drought and reflect the influences on North American drought related to Northern Hemisphere atmospheric and equatorial Pacific Ocean–atmospheric circulation, then time series of the two PCs could be used to show variations in the contribution of these two circulation patterns to North American drought over multidecadal time scales.

In assessing the most recent century in the context of the past six centuries, a prominent feature is the 1950s drought, for which PCs indicate both drought in the Southwest and in the western United States (Fig. 6a). This period of drought coincided with strong La Niña

conditions from 1954 to 1956 (Wolter and Timlin 1993), indicated by the deeply negative PC1, but also with negative PC2 loadings suggesting an additional influence. The most recent drought also shows a combination of negative values for the two PCs, but in this case the east–west PC shows a more negative loading. The early twentieth century is characterized by widespread and persistently wet conditions throughout much of the western United States (Fye et al. 2003; Woodhouse et al. 2005). Corresponding to this pluvial period is a peak in PC1 loadings, followed by a peak in PC2 loadings, suggesting that this wet period was first due to favorable conditions in the equatorial Pacific, followed by favorable conditions in Northern Hemisphere circulation. The strongly and persistently positive PC loadings for this period are unprecedented going back to at least 1400, in agreement with reconstructions of Colorado River flow for the past five centuries (Stockton and Jacoby 1976; Woodhouse et al. 2006), which is perhaps another indication of just how anomalous the hydroclimatic conditions were that formed the basis of Colorado River allocations.

The end of the sixteenth century has been noted for severe, persistent, and widespread drought conditions that occurred over many parts of North America (Woodhouse and Overpeck 1998; Stahle et al. 2000). It has been hypothesized that this drought was due to persistent La Niña conditions (Stahle et al. 2000). The loadings for PC1 are strongly negative for much of the second half of the sixteenth century, in agreement with a possible link to ENSO (Fig. 6a). However, PC2 loadings are also deeply negative within this period, indicating that west-wide drought was possibly also influenced by Northern Hemisphere circulation. PC2 shifts abruptly to positive values at the turn of the century and into the first part of the seventeenth century. The dry conditions in the eastern United States associated with positive loadings of PC2 are in good agreement with the documented drought in the early part of the seventeenth century that likely devastated the Jamestown Colony (Stahle et al. 1998). The Colorado River basin and other parts of the western United States were documented to be quite wet in the early seventeenth century, also in agreement with positive PC2 loadings (e.g., Fye et al. 2003; Cook et al. 2004; Woodhouse et al. 2006).

While the two PCs are only very weakly correlated at annual times scales ($r = 0.089$, 1404–2003), the decadally smoothed time series show a closer association between the two PCs after about 1620 (1404–1619, $r = 0.149$; 1620–2003, $r = 0.454$). This suggests that over the last four centuries, at decadal time scales, both circulation patterns may often contribute to the wet or dry conditions in areas with drought anomalies of the same sign in both PCs, such as in the U.S. intermountain west, the western Great Plains, and northern Mexico. This could also be an indication of periods when the relationship between tropical Pacific Ocean and Northern Hemisphere circulation is more closely linked. Before this time, which appears to be characterized by lower-frequency variability and more persistent drought, one pattern appears to dominate over the other at these time scales.

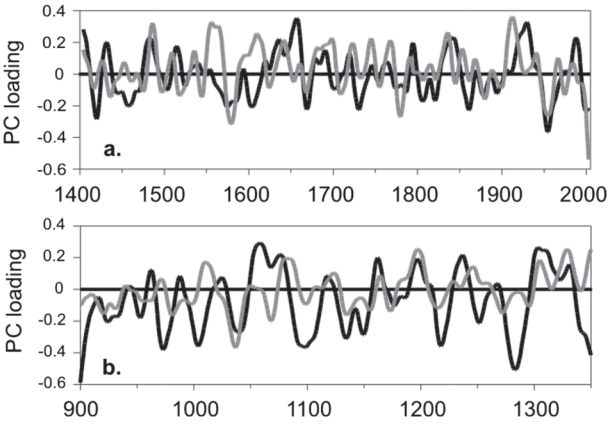

FIG. 6. Reconstructed PDSI loadings for PC1 (black line) and PC2 (gray line), smoothed with a 20-yr spline. Negative values of PC1 indicate a dry southwest–wet northwest, while negative values of PC2 indicate a dry west–wet east. Positive values indicate the opposite conditions: (a) 1404–2003 and (b) 900–1350.

During the Medieval period, the loadings of both PCs are often negative, with few extended periods of positive loadings (Fig. 6b). Periods when PCs are in and out of phase are also evident. The twelfth century has been shown to be a period of particularly persistent and widespread drought (Cook et al. 2004; Herweijer and Seager 2008; Meko et al. 2007). In this analysis, negative loadings on PC1 throughout much of the period, indicating drought in the Southwest (Fig. 6b), are in agreement with the studies that have suggested that a causal mechanism for the medieval droughts was a persistent La Niña state in the equatorial Pacific (Cook et al. 2007; Graham et al. 2007). During the medieval period, the percent of variance accounted for by PC1 more strongly suggests the role of ENSO (21% versus 14%) than in either the instrumental period (16% versus 14%) or the more recent reconstruction period (17% versus 18%), in support of previous work. In contrast, while the most persistent period of low flows in the Colorado River between A.D. 762–2005 is reported to be 1118–79 (Meko et al. 2007), and although this analysis suggests ENSO may have been a primary driver into the mid-1100s, neither PC is strongly negative after this point. The two PCs account for only 35% of the total variance, so other circulation features are likely influencing drought at this time period (as well as in other periods).

The numbers of chronologies from which the gridpoint PDSI is reconstructed is much reduced by 900. However, although sparsely distributed across the continent, regions west of the Rocky Mountains are still well represented, including the intermountain west, California, and the Pacific Northwest, with a small handful of eastern chronologies. Thus, the greater variance explained by PC1 during the medieval period is not likely to be due to a dominance of data in the southwestern United States. It should be noted that the comparisons of specific reconstructions with areas under drought are not independent, because virtually all of the tree-ring data have been used in the PDSI reconstructions as well as in the other reconstructions mentioned, but the point is that different circulation patterns may have lead to these regional droughts.

5. Conclusions

This analysis indicates two major patterns of drought across the U.S. and border regions of Canada and Mexico, a classic ENSO drought imprint and an east–west pattern of drought. The two patterns are remarkably robust over time, equally evident in both instrumental and reconstructed PDSI data, for the instrumental period as well as for the past six centuries. The two patterns are still well represented during the more data-scarce medieval period. The patterns seem to be insensitive to the number of components rotated, and composite maps using other sources of PDSI data display very similar patterns. The composite maps are based on the five years that best represent these patterns, and these patterns are supported by the mapped PC scores. In both cases, the resulting patterns are likely more clear-cut than will be the case in reality. The drought pattern for any given year will be a variable blend of the two PC patterns, in addition to other factors. The two patterns only explain about one-third of the total variance, indicating that complex and regional patterns more commonly characterize drought. However, this exercise serves as a starting point to investigate the circulation patterns associated with widespread drought patterns.

The 500-mb circulation patterns associated with the two drought patterns point to different types of circulation features related to drought. The circulation patterns by themselves cannot be interpreted as mechanistic features, but may be indicative of mechanisms. Although the PC1 drought pattern typifies the classic ENSO teleconnection pattern, especially in the western United States, the circulation pattern associated with this PC1 is not as clearly indicative of ENSO. The pattern also shares some features of the West Pacific index, which is related to equatorial Pacific conditions (Horel and Wallace 1981). Much research strongly supports the cool phase ENSO as a driver of drought in western North America, and it is likely that the link to ENSO exists here as well. The circulation associated with PC2 shares some of the main features of the Arctic Oscillation, which is part of a family of circulation modes that are characterized by opposing pressure in the northern middle and high latitudes, know collectively as the Northern Hemisphere annual mode (Thompson and Wallace 2000).

If these circulation patterns do indeed represent both tropical and Northern Hemisphere features, they suggest the role of both types of circulation in the occurrence of North American drought. Studies have suggested circulation typified by the NAM and ENSO are clearly important to midlatitude climate, so the link to major patterns of drought is plausible (Quadrelli and Wallace 2004; Nakamura et al. 2007). Because the two circulation modes are not independent (Nakamura et al. 2007), disentangling the influence of one or the other may be difficult. These results suggest that droughts in North America are influenced by the combined effects from the tropics and high latitudes, with one or the other playing a dominant role at times. Smoothed time series of the PC loadings indicate periods of time when the two are in phase and out of phase over decadal and multidecadal time scales. When in phase, the two patterns could be reinforcing the effects of each other, but may also indicate periods when the two circulation patterns are less independent. A challenge will be to confirm the findings suggested by this study in a way that provides a greater understanding of the drivers of drought under natural climate variability and global climate change.

Acknowledgments. Thanks to all the contributors of tree-ring chronologies that have made the reconstructed PDSI network possible, and to Ed Gille of the NOAA Paleoclimatology Branch for uploading the latest version of the PDSI reconstructions to run on the composite map tool. Our thanks also to Jeffery Lukas who helped with Fig. 3. We greatly appreciated the comments and suggestions of two anonymous reviewers.

REFERENCES

Arblaster, J., and Coauthors, 2007: Summary for policymakers. *Climate Change 2007: The Physical Science Basis,* S. Solomon et al., Eds., Cambridge University Press, 1–21.

Barlow, M., S. Nigam, and E. H. Berbery, 2001: ENSO, Pacific decadal variability, and U.S. summertime precipitation, drought, and stream flow. *J. Climate,* **14,** 2105–2128.

Barnston, A. G., and R. E. Livesey, 1987: Classification, seasonality, and persistence of low-frequency atmospheric circulation patterns. *Mon. Wea. Rev.,* **115,** 1083–1126.

Barry, R. G., and R. J. Chorley, 2003: *Atmosphere, Weather, and Climate*. 8th ed. Routledge, 421 pp.

Benson, L., and Coauthors, 2002: Holocene multidecadal and multicentennial droughts affecting Northern California and Nevada. *Quat. Sci. Rev.,* **21,** 659–682.

Blasing, T. J., 1975: Methods for analyzing climatic variations in the North Pacific sector and western North America for the last few centuries. Ph.D. dissertation, University of Wisconsin—Madison, 177 pp.

Brown, D. B., and A. C. Comrie, 2004: A winter precipitation 'dipole' in the western United States associated with multidecadal ENSO variability. *Geophys. Res. Lett.,* **31,** L09203, doi:10.1029/2003GL018726.

Cayan, D. R., 1996: Interannual climate variability and snow pack in the western United States. *J. Climate,* **9,** 928–948.

Cole, J. E., and E. R. Cook, 1998: The changing relationship between ENSO variability and moisture balance in the continental United States. *Geophys. Res. Lett.,* **25,** 4529–4532.

Cook, E. R., D. M. Meko, D. W. Stahle, and M. K. Cleaveland, 1999: Drought reconstructions for the continental United States. *J. Climate,* **12,** 1145–1162.

——, C. A. Woodhouse, C. M. Eakin, D. M. Meko, and D. W. Stahle, 2004: Long-term aridity changes in the western United States. *Science,* **306,** 1015–1018.

——, R. Seager, M. A. Cane, and D. W. Stahle, 2007: North American drought: Reconstructions, causes, and consequences. *Earth Sci. Rev.,* **81,** 93–134.

Dai, A., K. E. Trenberth, and T. Qian, 2004: A global data set of Palmer Drought Severity Index for 1870–2002: Relationship with soil moisture and effects of surface warming. *J. Hydrometeor.,* **5,** 1117–1130.

Daly, C., G. Taylor, and W. Gibson, 1997: The PRISM approach to mapping precipitation and temperature. *Proc. 10th Conf. on Applied Climatology,* Reno, NV, Amer. Meteor. Soc., 10–12.

Dettinger, M. D., D. R. Cayan, H. F. Diaz, and D. M. Meko, 1998: North–south precipitation patterns in western North America on interannual to decadal time scales. *J. Climate,* **11,** 3095–3111.

Diaz, H. F., 1983: Drought in the United States—Some aspects of major dry and wet periods in the contiguous United States, 1895–1981. *J. Climate Appl. Meteor.,* **22,** 3–16.

——, 1991: Some characteristics of wet and dry regimes in the contiguous United States: Implications for climate change detection efforts. *Greenhouse-Gas-Induced Climatic Change,* M. E. Schlesinger, Ed., Elsevier, 269–296.

Feng, S., R. J. Oglesby, C. M. Rowe, D. B. Loope, and Q. Hu, 2008: Atlantic and Pacific SST influences on Medieval drought in North America simulated by the Community Atmospheric Model. *J. Geophys. Res.,* **113,** D11101, doi:10.1029/2007JD009347.

Fye, F. K., D. W. Stahle, and E. R. Cook, 2003: Paleoclimatic analogs to 20th century moisture regimes across the USA. *Bull. Amer. Meteor. Soc.,* **84,** 901–909.

Gershunov, A., and T. P. Barnett, 1998: Interdecadal modulation of ENSO teleconnections. *Bull. Amer. Meteor. Soc.,* **79,** 2715–2725.

Glantz, M. R., R. W. Katz, and N. Nicholls, Eds., 1991: *Teleconnections Linking Worldwide Climate Anomalies*. Cambridge University Press, 545 pp.

Graham, N. E., and Coauthors, 2007: Tropical Pacific–mid-latitude teleconnections in medieval times. *Climatic Change,* **83,** 241–285, doi:10.1007/s10584-007-9239-2.

Herweijer, C., and R. Seager, 2008: The global footprint of persistent extra-tropical drought in the instrumental era. *Int. J. Climatol.,* **28,** 1761–1774, doi:10.1002/joc.1590.

——, ——, E. R. Cook, and J. Emile-Geay, 2007: North American droughts of the last millennium from a gridded network of tree-ring data. *J. Climate,* **20,** 1353–1376.

Horel, J. D., and J. M. Wallace, 1981: Planetary-scale atmospheric phenomena associated with the Southern Oscillation. *Mon. Wea. Rev.,* **109,** 813–829.

Kalnay, E., and Coauthors, 1996: The NCEP/NCAR 40-Year Reanalysis Project. *Bull. Amer. Meteor. Soc.,* **77,** 437–471.

Kangas, R. S., and T. J. Brown, 2007: Characteristics of U.S. drought and pluvials from a high-resolution spatial dataset. *Int. J. Climatol.,* **27,** 1303–1325.

Karl, T. R., 1983: Some spatial characteristics of drought duration in the United States. *J. Climate Appl. Meteor.,* **22,** 1356–1366.

——, and A. J. Koscielny, 1982: Drought in the United States: 1895-1981. *J. Climatol.,* **2,** 313–329.

McCabe, G. J., M. A. Palecki, and J. L. Betancourt, 2004: Pacific and Atlantic Ocean influences on multidecadal drought frequency in the United States. *Proc. Natl. Acad. Sci. USA,* **101,** 4136–4141.

Meko, D. M., C. A. Woodhouse, C. A. Baisan, T. Knight, J. J. Lukas, M. K. Hughes, and M. W. Salzer, 2007: Medieval drought in the upper Colorado River basin. *Geophys. Res. Lett.,* **34,** L10705, doi:10.1029/2007GL029988.

Nakamura, T., Y. Tachibana, and H. Shimoda, 2007: Importance of cold and dry surges in substantiating the NAM and ENSO relationship. *Geophys. Res. Lett.,* **34,** L22703, doi:10.1029/2007GL031220.

National Research Council, 2007: *Colorado River Basin Water Management: Evaluating and Adjusting to Hydroclimatic Variability*. National Academies Press, 222 pp.

NOAA/Climate Prediction Center, cited 2008: Monthly atmospheric and SST indices. [Available online at http://www.cpc.ncep.noaa.gov/data/indices/.]

NOAA/Earth System Research Laboratory, cited 2008: PSD interactive plotting and analysis pages. [Available online at http://www.cdc.noaa.gov/cgi-bin/data/getpage.pl.]

NOAA/National Climatic Data Center, cited 2008a: North American drought atlas PDSI reconstructions version 2a (2008)—Time series plots. [Available online at http://www.ncdc.noaa.gov/paleo/pdsi08_ts.html.]

——, cited 2008b: Tree-ring reconstructions of Palmer Drought Severity Index across North America over the last 2000 years. [Available online at http://www.ncdc.noaa.gov/cgi-bin/paleo/pd04plot.pl.]

——, cited 2008c: U.S. climate divisions dataset source and information. [Available online at http://www.cdc.noaa.gov/data/usclimdivs/data/.]

North, G. R., T. L. Bell, and R. F. Cahalan, 1982: Sampling errors in the estimation of empirical orthogonal functions. *Mon. Wea. Rev.,* **110,** 699–706.

Palmer, W. C., 1965: Meteorological drought. U.S. Weather Bureau Research Paper 45, 58 pp.

Quadrelli, R., and J. M. Wallace, 2004: Varied expressions of the hemispheric circulation observed in association with contrasting polarities of prescribed patterns of variability. *J. Climate,* **17,** 4245–4253.

Rajagopalan, B., E. Cook, U. Lall, and B. K. Ray, 2000: Spatiotemporal variability of ENSO and SST teleconnections to summer drought over the United States during the twentieth century. *J. Climate,* **13,** 4244–4255.

Rasmusson, E. G., and T. H. Carpenter, 1982: Variations in tropical sea surface temperature and surface wind fields associated with the Southern Oscillation/El Niño. *Mon. Wea. Rev.,* **110,** 354–384.

Redmond, K. T., and R. W. Koch, 1991: Surface climate and streamflow variability in the western United States and their relationship to large scale circulation indices. *Water Resour. Res.,* **27,** 2381–2399.

Richman, M. B., 1986: Rotation of principal components. *J. Climatol.,* **6,** 293–335.

Seager, R., Y. Kushnir, C. Herweijer, N. Naik, and J. Miller, 2005: Modeling of tropical forcing of persistent droughts and pluvials over western North America: 1856–2000. *J. Climate,* **18,** 4065–4088.

——, and Coauthors, 2007: Model projections of an imminent transition to a more arid climate in southwestern North America. *Science,* **316,** 1181–1184, doi:10.1126/science.1139601.

——, Y. Kushnir, M. F. Ting, M. Cane, N. Naik, and J. Velez, 2008: Would advance knowledge of 1930s SSTs have allowed prediction of the Dust Bowl drought? *J. Climate,* **21,** 3261–3281.

Shabbar, A., and W. Skinner, 2004: Summer drought patterns in Canada and the relationship to global sea surface temperatures. *J. Climate,* **17,** 2866–2880.

Stahle, D. W., M. K. Cleaveland, D. B. Blanton, M. D. Therrell, and D. A. Gay, 1998: The Lost Colony and Jamestown droughts. *Science,* **280,** 564–567.

——, E. R. Cook, M. K. Cleaveland, M. D. Therrell, D. M. Meko, H. D. Grissino-Mayer, E. Watson, and B. H. Luckman, 2000: Tree-ring data document 16th century megadrought over North America. *Eos, Trans. Amer. Geophys. Union,* **81,** 121.

StatSoft, Inc., 2005: STATISTICA (data analysis software system), version 7.1. [Available online at http://www.statsoft.com.]

Stockton, C. W., and G. C. Jacoby, 1976: Long-term surface-water supply and streamflow trends in the Upper Colorado River Basin. *Lake Powell Research Project Bulletin 18,* National Science Foundation, 73 pp.

Thompson, D. W. J., and J. M. Wallace, 1998: The Arctic Oscillation signature in the wintertime geopotential height and temperature fields. *Geophys. Res. Lett.,* **25,** 1297–1300.

——, and ——, 2000: Annular modes in the extratropical circulation. Part I: Month-to-month variability. *J. Climate,* **13,** 1000–1016.

Wallace, J. M., and D. S. Gutzler, 1981: Teleconnections in the geopotential height field during the Northern Hemisphere winter. *Mon. Wea. Rev.,* **109,** 784–812.

Wolter, K., and M. S. Timlin, 1993: Monitoring ENSO in COADS with a seasonally adjusted principal component index. *Proc. of the 17th Climate Diagnostics Workshop,* Norman, OK, NOAA/NMC/CAC and Cosponsors, 52–57.

Woodhouse, C. A., and J. T. Overpeck, 1998: 2000 years of drought variability in the central United States. *Bull. Amer. Meteor. Soc.,* **79,** 2693–2714.

——, K. E. Kunkel, D. R. Easterling, and E. R. Cook, 2005: The twentieth-century pluvial in the western United States. *Geophys. Res. Lett.,* **32,** L07701, doi:10.1029/2005GL022413.

——, S. T. Gray, and D. M. Meko, 2006: Updated streamflow reconstructions for the Upper Colorado River basin. *Water Resour. Res.,* **42,** W05415, doi:10.1029/2005WR004455.

Yarnal, B., 1993: *Synoptic Climatology in Environmental Analysis: A Primer*. Belhaven Press, 256 pp.